Supplement of Geosci. Model Dev., 16, 5493–5514, 2023
https://doi.org/10.5194/gmd-16-5493-2023-supplement

Geoscientific Model Development
Open Access
EGU

Supplement of

Evaluating WRF-GC v2.0 predictions of boundary layer height and vertical ozone profile during the 2021 TRACER-AQ campaign in Houston, Texas

Xueying Liu et al.

Correspondence to: Yuxuan Wang (ywang246@central.uh.edu)

Text S1. Identification of ozone episodes

Ozone exceedance days were identified according to surface measurements from the TCEQ CAMS (onshore) and the boats operating in Galveston Bay during the field campaign (offshore). Full description of the boat observations is given in Li et al. (2023). The criteria used in this study are (1) any onshore site from the CAMS network in Houston and Galveston or (2) offshore boat ozone observations that registered daily maximum 8-hour average (MDA8) ozone in exceedance of 70 ppbv, the current air quality standard for ozone. In total, six ozone episodes were identified during the whole campaign period over July-Oct 2021 (Table S1). Among these, three ozone episodes are in the extensive operating period of September 2021.

Table S1. Dates of ozone episodes and the associated MDA8 O_3 maximum.

Episodes	Highest MDA8 O_3 (ppbv)	
	Onshore (CAMS)	Offshore (Boat)
07/26 - 07/28	97	72
08/25	78	50
09/06 - 09/11	89	79
09/17 - 09/19	75	80
09/23 - 09/26	81	65
10/06 - 10/09	92	96

Text S2. Description of WRF nudging

We used observation nudging together with surface analysis nudging (also known as surface grid nudging) in WRF as the data assimilation method. In observation nudging, the modeled fields are nudged to match better with observations at individual locations with a radius of influence. The data used for observation nudging are ground-based hourly measurements of temperature, relative humidity as well as wind speed and direction from the Texas Commission on Environmental Quality (TCEQ) continuous ambient monitoring stations (CAMS). Based on site elevations, most nudging is performed within 500 m above sea level in eastern Texas, as shown in Figure S1. There are around 155, 98, and 49 observations ingested into WRF domains 1, 2 and 3, respectively. In analysis nudging, temperature, moisture and wind fields are nudged toward gridded analysis above the PBL (~1 km). The OBSGRID program was used for both observation nudging and surface analysis nudging. The program generated merged input files so that observation nudging and surface analysis nudging were conducted simultaneously when running the model. In addition to data assimilation, we adopted objective analysis in OBSGRID to provide better initial and boundary conditions, where first-guess meteorological fields are updated by incorporating observational data. The combined adoption of observation nudging, surface analysis nudging, and objective analysis in the [Nudged] simulation was to maximize the benefits of assimilating observations, as recommended by Chapter 7 of the WRF user guide.

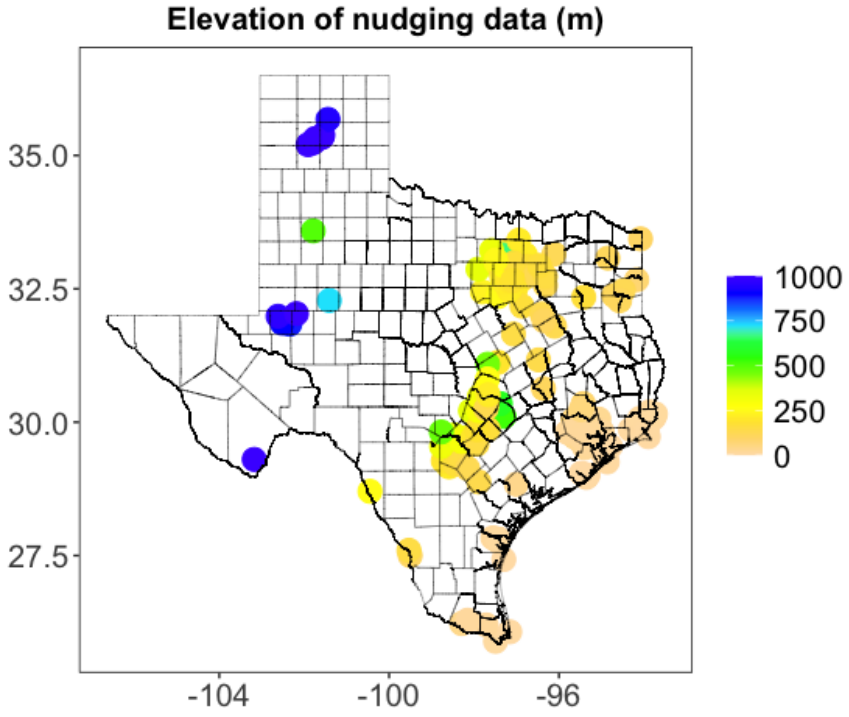

Figure S1. Elevation of the Texas Commission on Environmental Quality (TCEQ) continuous ambient monitoring stations (CAMS) used as observational data for WRF nudging methods.

Text S3. Evaluation of all model experiments

All WRF simulations are shown in Table S2. We evaluated the spatial and temporal variabilities of all simulations against the onshore TCEQ CAMS (Figure S2; Figure S3; Table S3) and the offshore boat measurements (Figure S4; Figure S5; Table S4). The WRF model generally reproduces observed temporal variability and spatial distribution in key meteorological parameters with a correlation coefficient higher than 0.5 in most cases. However, the model, regardless of configuration settings, shows persistent low biases in PBL heights, low biases in air temperatures, high biases in relative humidity, and high biases in wind speed. While different WRF configuration has its own advantage in reducing model biases, [HRRR], [Nudged] and [Reinit] configurations stand out as the three best simulations based on campaign-wide statistics. Considering that [Nudged] requires additional efforts to prepare observational datasets and [Reinit] needs to automate the model running process, [HRRR] is the easiest and the most effective option to reproduce meteorology for computationally expensive chemistry simulations and was thus selected to be presented in the main text.

Table S2. List of model experiments.

Simulations	BC Meteorology	PBL	Microphysics	Nudging	Reinitializing
[Base]	NCEP FNL	MYNN	2M	No	No
[WSM6]	NCEP FNL	MYNN	WSM6	No	No
[YSU]	NCEP FNL	YSU	2M	No	No
[ACM2]	NCEP FNL	ACM2	2M	No	No
[ERA5]	ECMWF ERA5	MYNN	2M	No	No
[HRRR]	HRRR	MYNN	2M	No	No
[Nudged]	NCEP FNL	MYNN	2M	Yes	No
[Reinit]	NCEP FNL	MYNN	2M	No	Yes

The mean of wind speed and direction is calculated using the vector notation approach, a commonly used method in wind evaluations, as described in Yu et al. (2023). This method treats wind as vectors with their u (eastward) and v (northward) wind components. First, the mean u and v wind components are found by averaging all u and v wind values over a given time period. Then, the resultant vector is determined by taking the square root of the sum of the squares of the mean u and mean v wind components. The magnitude of resultant vector represents the mean wind speed, and the angle of the resultant vector represents the mean wind direction.

The difference between observed and modeled wind direction was calculated as below.

$$\Delta = \begin{cases} M - O, & \text{when } |M - O| \le 180^\circ \\ (M - O)\left(1 - \dfrac{360}{|M - O|}\right), & \text{when } |M - O| > 180^\circ \end{cases}$$

where M is the model output, and O is the observation. The correlation between observed and modeled wind direction was determined by a circular correlation coefficient as below.

$$R = \frac{\sum_{i=1}^{N} \sin\,(M_i - \bar{M}) \sin\,(O_i - \bar{O})}{\sqrt{\sum_{i=1}^{N} \sin^2(M_i - \bar{M})} \sqrt{\sum_{i=1}^{N} \sin^2(O_i - \bar{O})}}$$

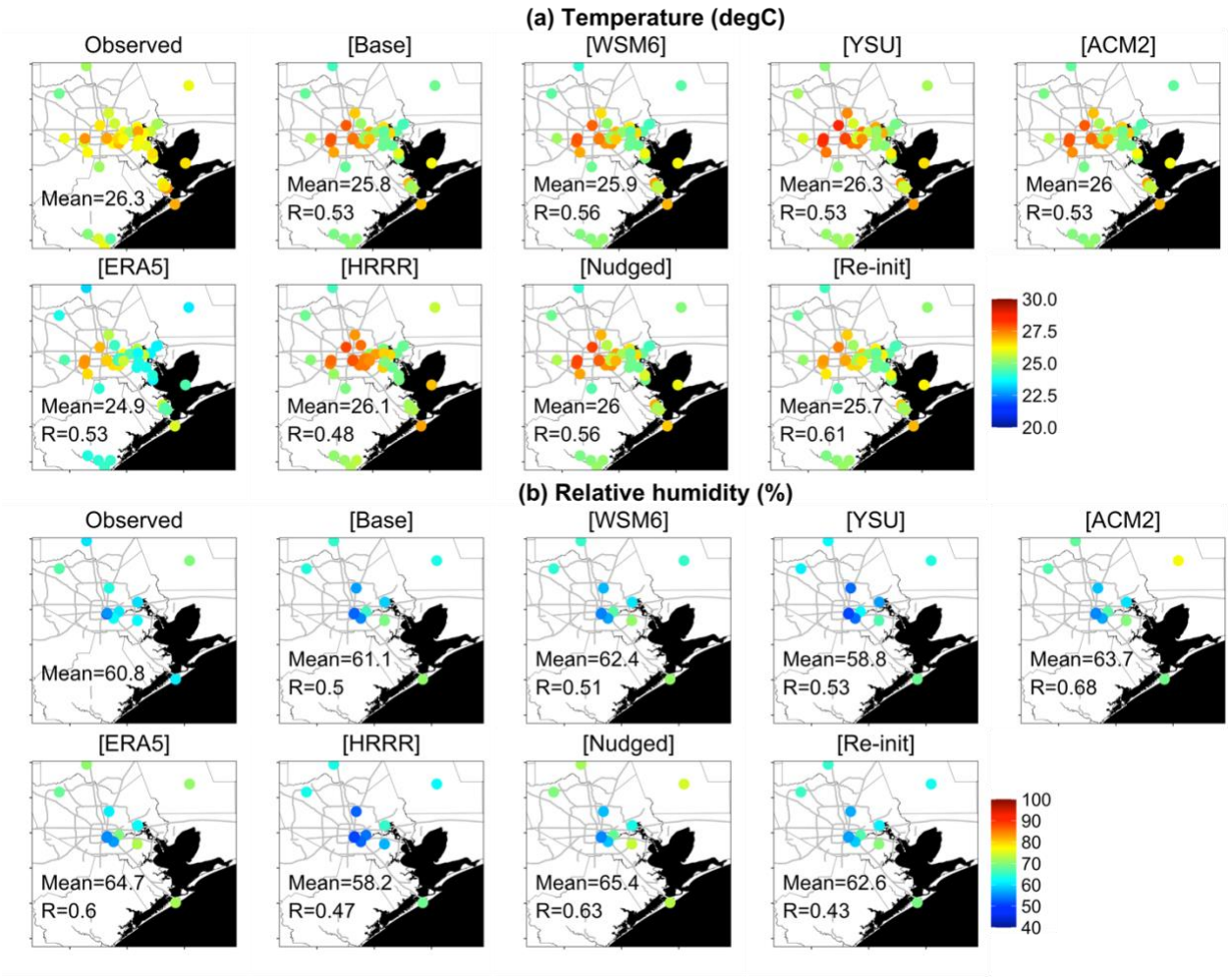

Figure S2. Spatial distribution of temporal averages of CAMS-observed and modeled mean meteorology during ozone episodes. The averages of wind speed and directions are calculated using the directional and vector mean approach. First, the mean of the u-wind (and v-wind) component is computed by averaging all u-wind (and v-wind) values at each station over the given period of time. Then, the mean wind speed and direction are calculated based on these mean u and v wind components at each station.

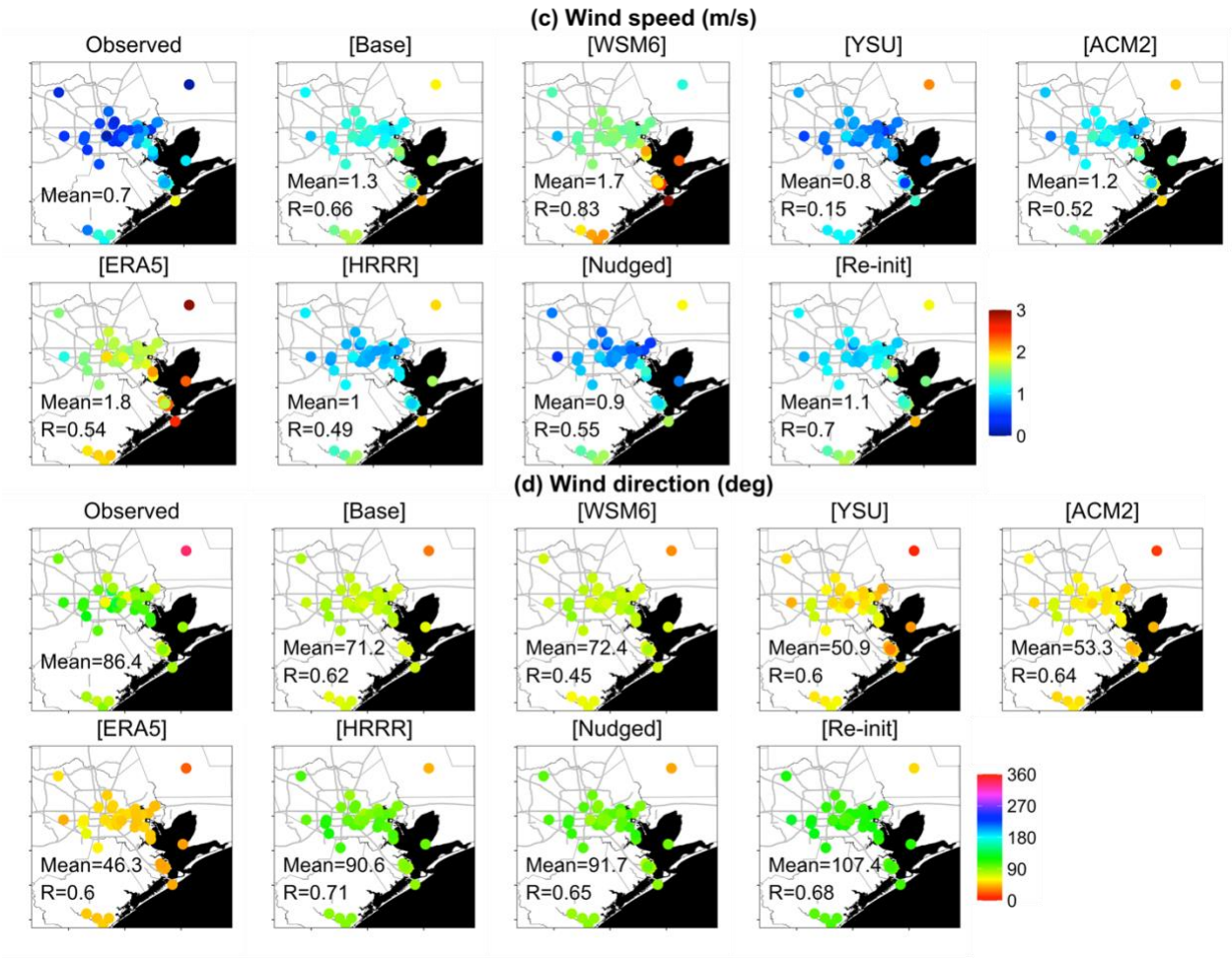

Figure S2 (continued). Spatial distribution of temporal averages of CAMS-observed and modeled mean meteorology during ozone episodes. The averages of wind speed and directions are calculated using the directional and vector mean approach. First, the mean of the u-wind (and v-wind) component is computed by averaging all u-wind (and v-wind) values at each station over the given period of time. Then, the mean wind speed and direction are calculated based on these mean u and v wind components at each station.

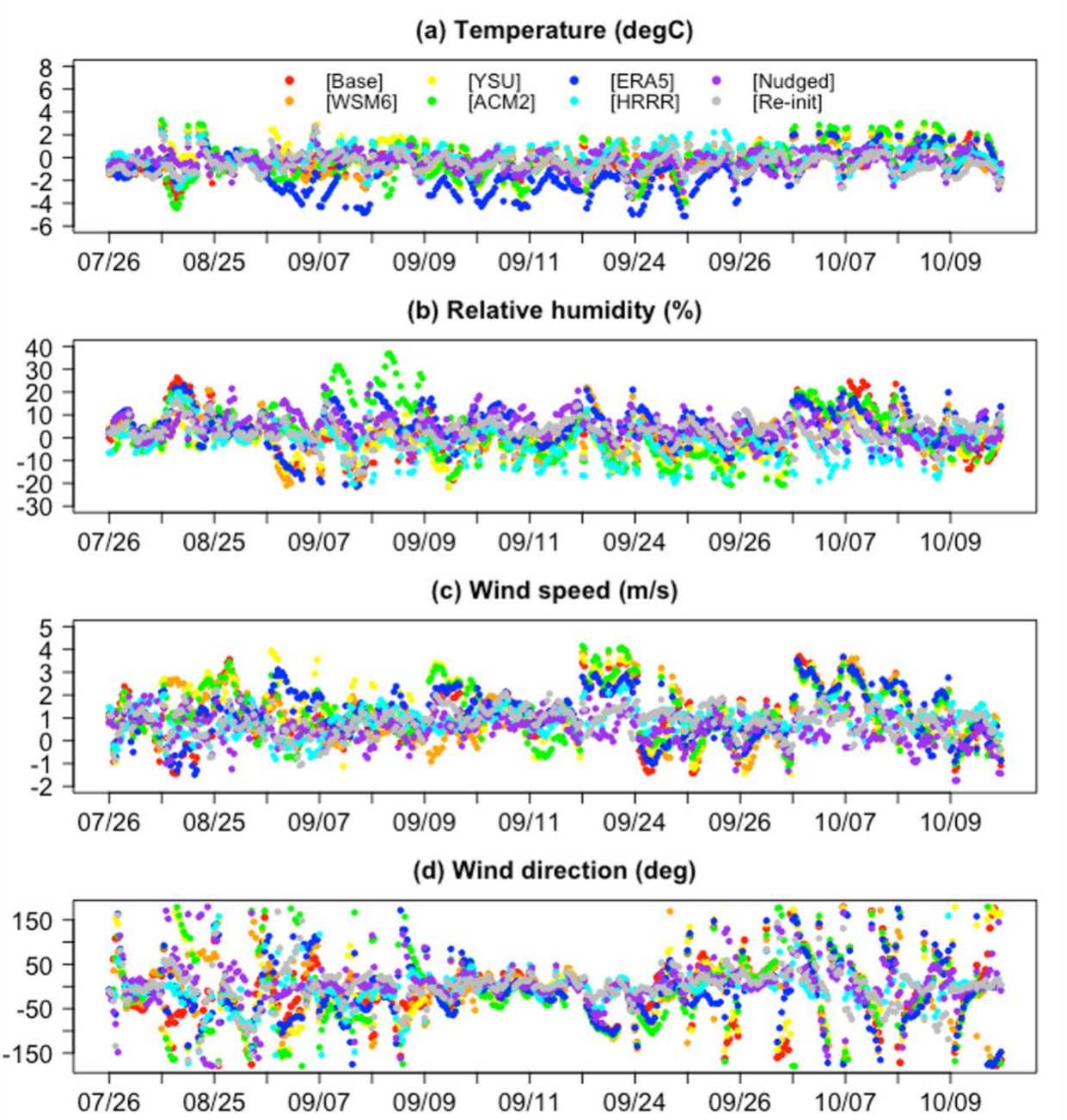

Figure S3. Hourly time series of observation-model differences (i.e., model minus observation) are shown for (a) air temperature, (b) relative humidity, (c) wind speed and (d) wind direction. The differences are spatial averages across all CAMS stations and the WRF model equivalents during ozone episodes. Refer to Text S3 for the calculations of spatial averages of wind speed and directions, as well as the differences between observed and modeled wind directions.

Table S3. Performance metrics of spatiotemporal variability between CAMS-observed and WRF-modeled meteorology during ozone episodes. Hourly meteorology at all stations is used for the calculation of performance metrics below. All metrics have the same unit as meteorological variables, except that the correlation coefficient (R) and normal mean bias (NMB) are unitless. OBS and MOD represent the spatial and temporal averages of observations and model equivalents, respectively.

Variables	Simulation	OBS	MOD	R	NMB	MB	MAE	RMSE
Temperature (°C)	[Base]	26.18	25.82	0.88	-0.01	-0.36	1.69	2.15
	[WSM6]		25.84	0.89	-0.01	-0.35	1.57	1.99
	[YSU]		26.29	0.89	0.00	0.11	1.65	2.11
	[ACM2]		25.95	0.86	-0.01	-0.23	1.76	2.23
	[ERA5]		24.91	0.85	-0.05	-1.28	2.17	2.71
	[HRRR]		26.12	0.89	0.00	-0.06	1.59	2.05
	[Nudged]		25.92	0.92	-0.01	-0.26	1.43	1.84
	[Re-init]		25.69	0.92	-0.02	-0.49	1.41	1.77
Relative humidity (%)	[Base]	60.12	60.94	0.76	0.01	0.82	10.25	13.04
	[WSM6]		62.21	0.78	0.03	2.09	9.85	12.28
	[YSU]		58.45	0.80	-0.03	-1.68	9.54	12.31
	[ACM2]		62.73	0.71	0.04	2.60	11.40	14.71
	[ERA5]		64.21	0.77	0.07	4.08	10.55	12.76
	[HRRR]		57.82	0.79	-0.04	-2.30	9.13	12.13
	[Nudged]		64.63	0.82	0.08	4.51	9.54	12.05
	[Re-init]		62.57	0.84	0.04	2.45	8.37	10.66
Wind speed (m/s)	[Base]	0.67	1.29	0.35	0.59	1.01	1.40	1.70
	[WSM6]		1.67	0.37	0.61	1.04	1.39	1.72
	[YSU]		0.80	0.39	0.75	1.29	1.55	1.87
	[ACM2]		1.16	0.38	0.66	1.12	1.44	1.77
	[ERA5]		1.76	0.43	0.64	1.09	1.38	1.66
	[HRRR]		1.00	0.54	0.49	0.83	1.12	1.36
	[Nudged]		0.89	0.55	0.30	0.51	0.96	1.20
	[Re-init]		1.14	0.61	0.48	0.82	1.07	1.31
Wind direction (deg)	[Base]	87.76	72.32	0.43	-0.05	-7.67	56.5	73.36
	[WSM6]		72.56	0.38	-0.04	-5.51	56.41	72.93
	[YSU]		53.26	0.41	-0.08	-12.14	60.30	77.29
	[ACM2]		54.87	0.37	-0.07	-10.64	64.15	81.29
	[ERA5]		47.32	0.43	-0.07	-10.92	58.05	74.83
	[HRRR]		92.51	0.61	-0.02	-3.43	40.16	57.55
	[Nudged]		93.29	0.48	0.02	3.00	46.05	64.70
	[Re-init]		109.03	0.47	0.00	-0.32	39.99	57.67

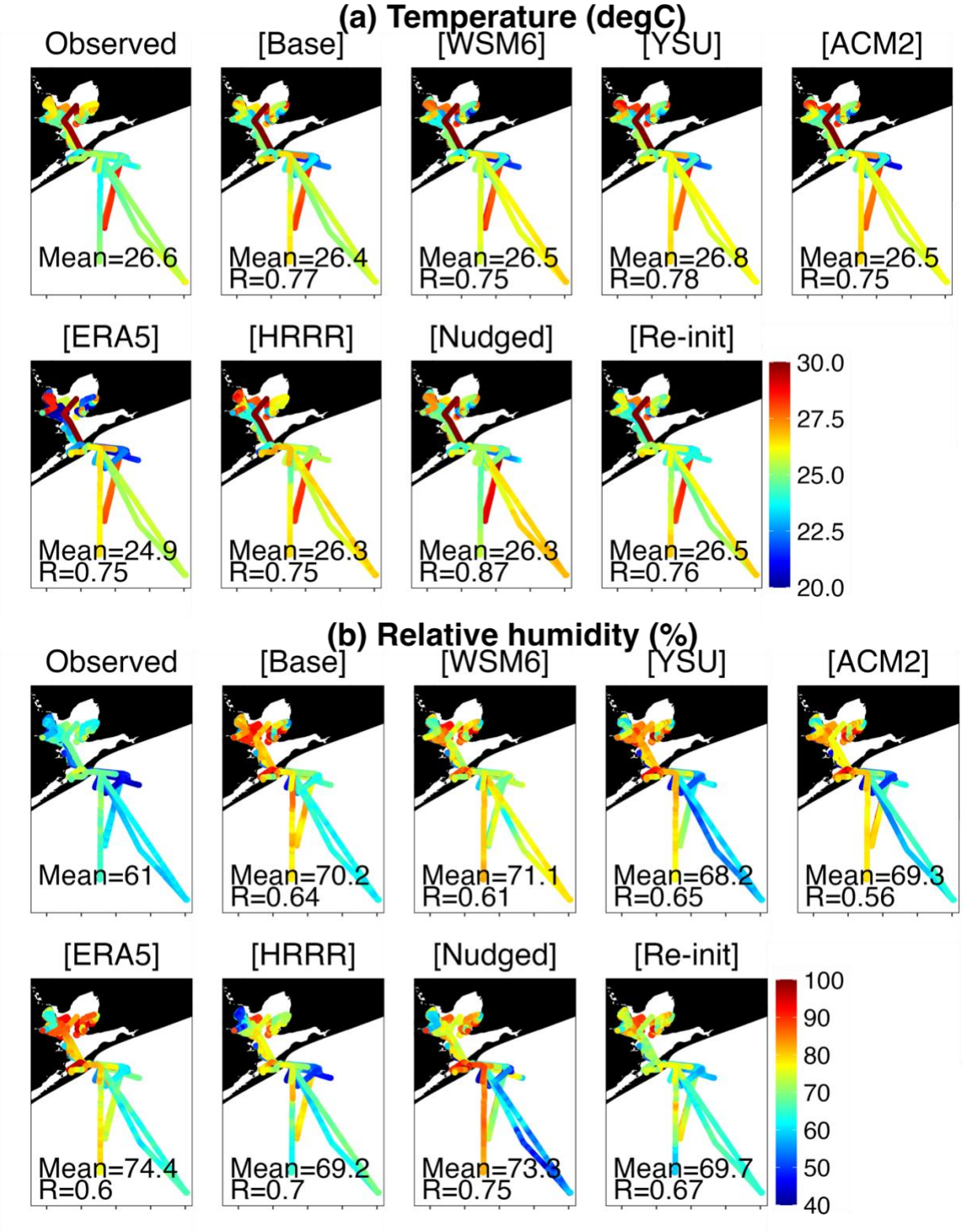

Figure S4. Spatial distribution of boat-observed and modeled meteorology during ozone episodes.

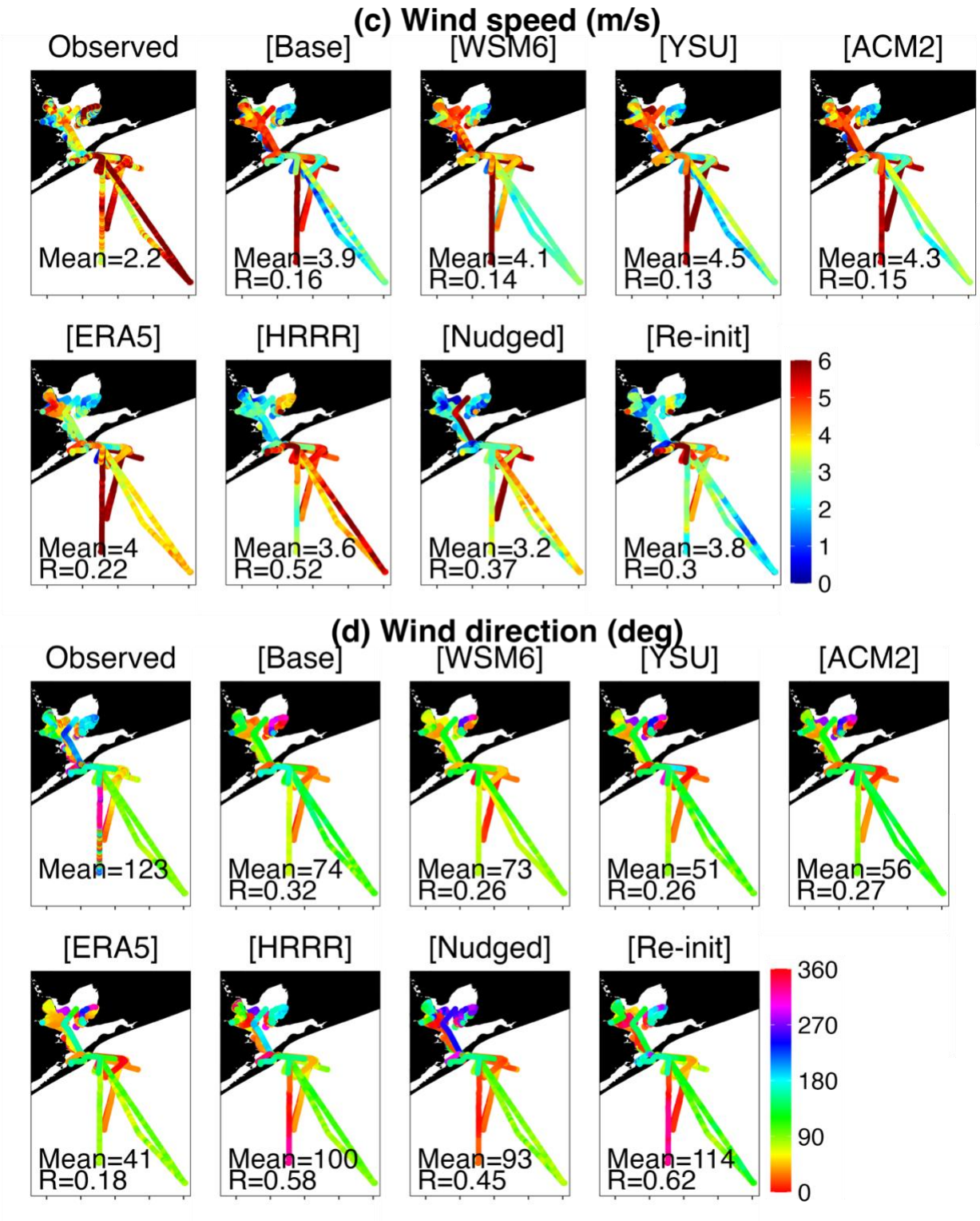

Figure S4 (continued). Spatial distribution of boat-observed and modeled meteorology during ozone episodes.

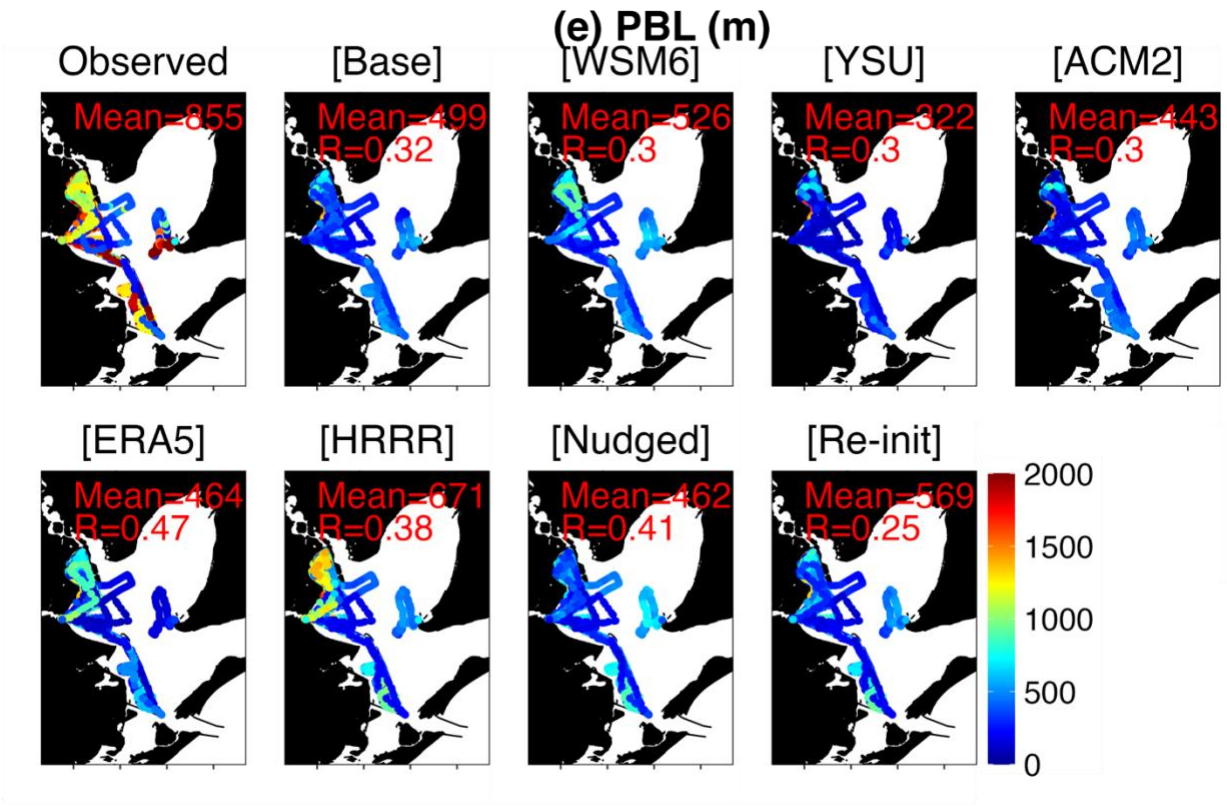

Figure S4 (continued). Spatial distribution of boat-observed and modeled meteorology during ozone episodes.

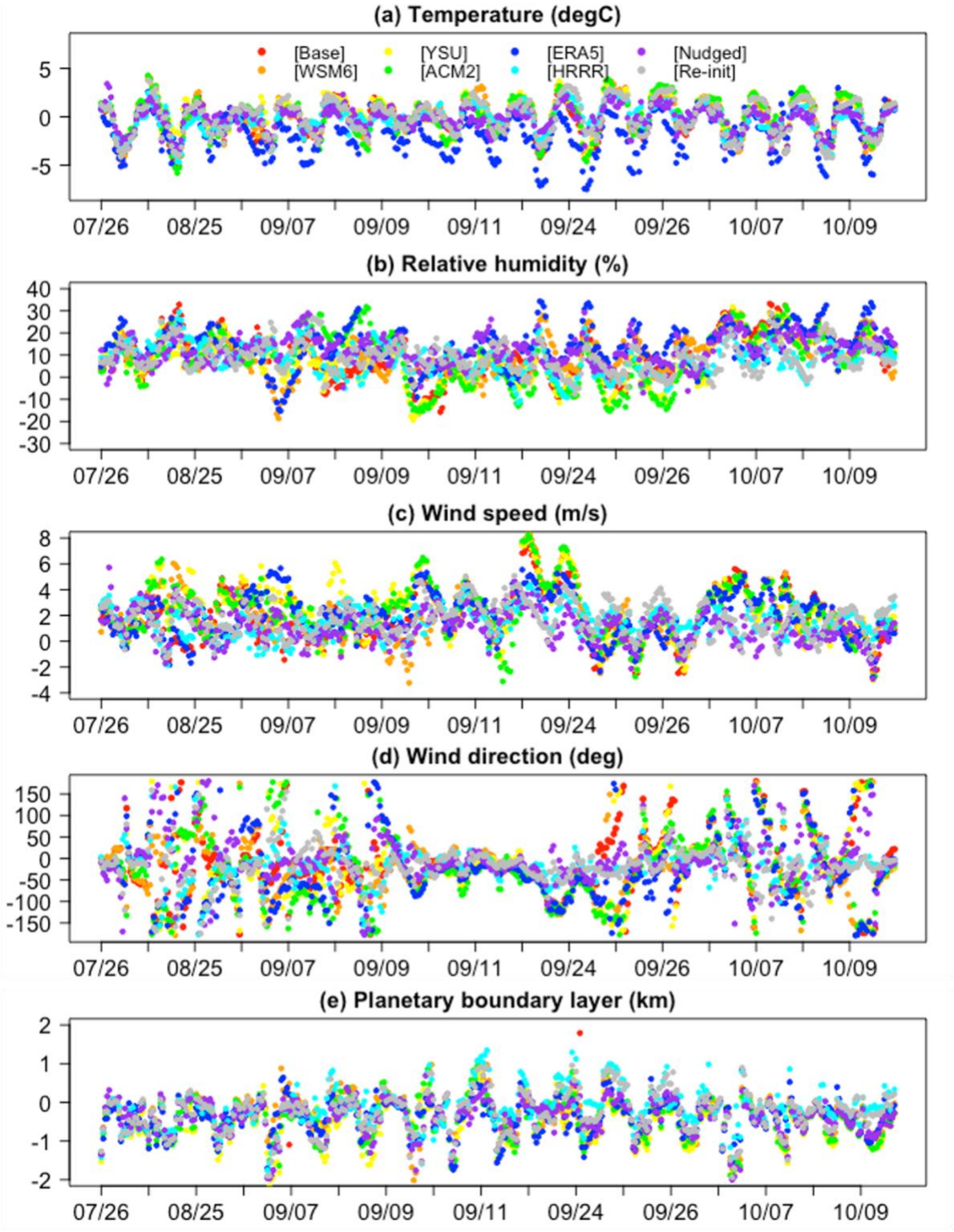

Figure S5. Hourly time series of observation-model differences (i.e., model minus observation) are shown for (a) air temperature, (b) relative humidity, (c) wind speed, (d) wind direction and (e) boundary layer height during ozone episodes. Refer to Text S3 for the calculations of averages of wind speed and directions, as well as the differences between observed and modeled wind directions.

Table S4. Performance metrics of spatiotemporal variability between boat-observed and WRF-modeled meteorology during ozone episodes. 1-minute meteorology is used for the calculation of performance metrics below. All metrics have the same unit as meteorological variables, except that the correlation coefficient (R) and normal mean bias (NMB) are unitless. OBS and MOD represent the spatial and temporal averages of observations and model equivalents, respectively.

Variables	Simulation	OBS	MOD	R	NMB	MB	MAE	RMSE
Temperature (°C)	[Base]	26.55	26.45	0.77	0.00	-0.11	1.71	2.14
	[WSM6]		26.50	0.75	0.00	-0.05	1.77	2.20
	[YSU]		26.78	0.78	0.01	0.22	1.71	2.10
	[ACM2]		26.51	0.75	0.00	-0.04	1.78	2.21
	[ERA5]		24.85	0.75	-0.06	-1.70	2.21	3.00
	[HRRR]		26.30	0.75	-0.01	-0.25	1.89	2.29
	[Nudged]		26.30	0.87	-0.01	-0.25	1.26	1.65
	[Re-init]		26.53	0.76	0.00	-0.02	1.71	2.15
Relative humidity (%)	[Base]	60.96	70.24	0.64	0.15	9.28	11.95	14.59
	[WSM6]		71.09	0.61	0.17	10.14	11.76	14.38
	[YSU]		68.20	0.65	0.12	7.24	10.96	13.29
	[ACM2]		69.35	0.56	0.14	8.40	12.75	15.33
	[ERA5]		74.38	0.60	0.22	13.42	14.66	17.23
	[HRRR]		69.20	0.70	0.14	8.24	10.38	12.68
	[Nudged]		73.35	0.75	0.20	12.39	12.87	14.92
	[Re-init]		69.68	0.67	0.14	8.72	10.25	12.42
Wind speed (m/s)	[Base]	0.73	2.47	0.16	0.74	1.67	2.20	2.78
	[WSM6]		2.62	0.14	0.82	1.85	2.33	2.92
	[YSU]		2.17	0.13	0.99	2.22	2.63	3.19
	[ACM2]		1.99	0.15	0.92	2.07	2.49	3.09
	[ERA5]		1.89	0.22	0.78	1.74	2.21	2.72
	[HRRR]		1.68	0.52	0.59	1.32	1.69	2.05
	[Nudged]		1.75	0.37	0.41	0.92	1.57	1.96
	[Re-init]		2.02	0.30	0.69	1.55	2.00	2.41
Wind direction (deg)	[Base]	144.15	118.78	0.32	-0.08	-11.45	57.74	75.38
	[WSM6]		113.5	0.26	-0.13	-19.10	60.40	77.29
	[YSU]		135.77	0.26	-0.11	-16.44	63.52	81.13
	[ACM2]		125.25	0.27	-0.11	-17.20	68.93	85.92
	[ERA5]		96.69	0.18	-0.17	-25.20	69.00	85.30
	[HRRR]		137.93	0.58	-0.08	-12.53	41.54	58.16
	[Nudged]		146.95	0.45	-0.05	-7.68	47.87	65.51
	[Re-init]		146.96	0.62	-0.10	-14.98	42.98	59.66
	[Base]	855.58	499.27	0.32	-0.42	-356.30	529.63	699.67

Boundary layer height (m)	[WSM6]		526.69	0.30	-0.38	-328.88	526.38	691.82
	[YSU]		322.22	0.30	-0.62	-533.36	612.29	817.16
	[ACM2]		443.60	0.30	-0.48	-411.97	562.12	747.06
	[ERA5]		464.75	0.47	-0.46	-390.83	507.51	680.30
	[HRRR]		671.27	0.38	-0.22	-184.31	461.30	637.68
	[Nudged]		462.09	0.41	-0.46	-393.48	516.18	696.37
	[Re-init]		569.57	0.25	-0.33	-286.00	518.21	689.22

References:

Li, W., Wang, Y., Liu, X., Soleimanian, E., Griggs, T., Flynn, J., and Walter, P.: Understanding offshore high-ozone events during TRACER-AQ 2021 in Houston: Insights from WRF-CAMx photochemical modeling, EGUsphere [preprint], https://doi.org/10.5194/egusphere-2023-1117, 2023.

Yu, E., Bai, R., Chen, X., and Shao, L.: Impact of physical parameterizations on wind simulation with WRF V3.9.1.1 under stable conditions at planetary boundary layer gray-zone resolution: a case study over the coastal regions of North China, Geosci. Model Dev., 15, 8111–8134, https://doi.org/10.5194/gmd-15-8111-2022, 2022.